Two types of electron microscopy analyses were combined with passive sampling and geographic information system mapping to investigate airborne particle sources in desert cities.

Spectral Imaging and Passive Sampling to Investigate Particle Sources in Urban Desert Regions

Jeff Wagner*
California Department of Public Health, Environmental Health Laboratory Branch, 850 Marina Bay Parkway, G365/EHLB, Richmond, CA 94804
jeff.wagner@cdph.ca.gov

Gary S. Casuccio
RJ Lee Group, Inc. 350 Hochberg Road, Monroeville, PA 15146
gcasuccio@rjleegroup.com

*corresponding author

Keywords: windblown dust, PM10, electron microscopy, UNC Passive sampler, CCSEM, GIS

Submitted to *Environmental Science: Processes & Impacts* February 2014
Revised manuscript submitted April 2014

ABSTRACT

Two types of electron microscopy analyses were employed along with geographic information system (GIS) mapping to investigate potential sources of $PM_{2.5}$ and PM_{10} (airborne particulate matter smaller than 2.5 and 10 μm, respectively) in two urbanized desert areas known to exhibit PM excursions. Integrated spectral imaging maps were obtained from scanning electron microscopy/energy-dispersive x-ray spectroscopy (SEM/EDS) analyses of 13 filters collected in Imperial Valley, California. Seven were from 24-hr PM_{10} Federal Reference Method (FRM) samplers and six were from $PM_{2.5}$ FRM samplers. This technique enabled extraction of information from particles collected on complex filter matrices, and indicated that all samples exhibited substantial proportions of crustal particles. Six Imperial $PM_{2.5}$ and PM_{10} filters selected from unusually high-PM days exhibited more large particles (2.5-15 and 10-30 μm, respectively) than did filters from low-PM days, and were more consistent with soils analyzed from the region. High winds were present on three of the six high-PM days. One of the high-$PM_{2.5}$ filters also exhibited substantial fine carbonaceous soot PM, suggesting significant contributions from a combustion source. Computer-controlled SEM/EDS (CCSEM/EDS) was conducted on PM collected with UNC Passive samplers from Phoenix, Arizona. The passive samplers showed good agreement with co-located FRM PM_{10} and $PM_{2.5}$ measurements (μg/m^3), and also enabled detailed individual particle analysis. The CCSEM/EDS data revealed mostly crustal particles in both the Phoenix fine and coarse PM_{10} fractions. GIS maps of multiple dust-related parameters confirm that both Imperial Valley and Phoenix possess favorable conditions for airborne crustal PM from natural and anthropogenic sources.

ENVIRONMENTAL IMPACT

Effectively assessing and controlling community exposures to airborne particulate matter (PM) requires knowledge of PM sources, composition and aerodynamic size. Conventional analyses of Federal Reference Method (FRM) PM samples typically allow only limited PM characterization. In this study, two types of electron microscopy analyses were employed along with geographic information system (GIS) mapping to gain better insight into PM sources affecting desert cities. Spectral imaging maps obtained from scanning electron microscopy with energy dispersive spectroscopy (SEM/EDS) were used to extract qualitative chemical and size information from particles collected on FRM filter matrices. Computer-controlled SEM/EDS (CCSEM/EDS) was conducted on co-located UNC Passive PM samplers to yield more detailed measurements of individual particles, mass concentrations (μg/m^3), and size distributions.

INTRODUCTION

Effectively assessing and controlling community exposures to airborne particulate matter (PM) requires knowledge of PM sources, composition and aerodynamic size. Conventional bulk analyses of US EPA Federal Reference Method (FRM) PM samples do not permit individual particle analysis and thus enable only limited PM characterizations. Scanning electron microscopy plus energy-dispersive x-ray spectroscopy (SEM/EDS) is a powerful tool for characterizing individual particle size, morphology, and composition, but the complexity of FRM filter matrices makes SEM/EDS analyses challenging. Spectral imaging (SI) mapping is a SEM/EDS technique in which elemental chemistry data is acquired and stored along with each image pixel. Composition maps may then be created across entire images or selected areas, a potentially useful technique for sample intercomparisons and individual particle analyses on FRM filter matrices.

Table 1. Sampling information for 24-hr FRM filter samples from Imperial Valley.

Filter ID	Location	Filter Date	PM Class ($\mu g/m^3$)	Wind Class (hrs with avg. >20 MPH)
PM_{10} filters				
1H	A	9/8/06	High (180)	Low (0)
1L1	B	9/8/06	Low (75)	Low (0) [b]
1L2	A	4/29/06	Low (25)	Low (0)
2H	C	5/9/11	High (220)	High (22)
2L1	C	5/15/11	Low (56)	High (16)
2L2	A	5/9/11	Low (45)	High (4)
2L3	A	5/15/11	Low (52)	High (1)
$PM_{2.5}$ filters				
3H	D	3/31/12	High (56)	High (1)
3L	D	4/3/12	Low (11)	Low (0)
4H	D	5/25/12	High (120)	High (4)
4L	D	5/27/12	Low (14)	Low (0)
5H	D	6/28/10	High (41) [a]	Low (0)
6H	D	10/15/11	High (41) [a]	Low (0)

[a]no comparison low-PM filters obtained.
[b] wind data obtained from station 5 mi away.

Co-location of UNC Passive PM samplers (1) can potentially provide further insight into ambient PM. These samplers are well-suited for computer-controlled SEM/EDS (CCSEM/EDS) analysis, which can measure individual size and composition data for of hundreds to thousands of particles per sample (2). In addition, inexpensive, passive samplers require less effort to deploy and operate than active, FRM samplers, which require maintenance, calibrated pumps, and electrical power on site. The use of multiple passive samplers enables PM measurement simultaneously at several locations, which can assist in the identification of local and regional sources (3).

Improved PM characterization is of interest in both Imperial Valley, California and Phoenix, Arizona, two Southwestern US (PM with aerodynamic diameters nominally smaller than 10 μm) (4). Natural and anthropogenic sources of airborne dust are important potential PM contributors in these two regions, both of which consist of desert and agricultural lands surrounding urbanized areas. The dramatic dust storms which occur occasionally in the Phoenix area are an unambiguous example of PM excursions dominated by windblown dust (5), while crop burning, construction, and highway vehicles are important candidate sources in more routine conditions (6) (7). Windblown dust erosion has been shown to impact health, visibility, and agricultural productivity, and is significantly correlated with livestock grazing intensity, tilling methods, crop selection, and vehicle speeds on roads (8) (9) (10) (11) (12).

In this study, we acquired SI maps from FRM PM_{10} and $PM_{2.5}$ filters collected in Imperial Valley to determine particle chemistry and size characteristics and identify potential sources. We also conducted CCSEM/EDS analyses of passive UNC PM samplers co-located with FRM samplers in Phoenix to obtain more detailed chemical and size information from individual particles. Geographic information system (GIS) mapping of dust-related parameters was employed to help interpret the results.

METHODS

Environmental Sampling

Thirteen filters were obtained from 24-hr FRM samplers at four monitoring network locations in Imperial Valley 2006-12 (Table 1). Six were 37-mm PTFE $PM_{2.5}$ filters from a 16.7 LPM R&P 2025 Sampler; the remaining seven were 8x10" quartz-fiber PM_{10} filters from Hi-vol (1130 LPM) SA 1200 Samplers. Six of these filters were selected from unusually high-PM days, and four of them were matched with low-PM filters from different days and/or nearby sites on the same sampling days. PM data and resultant winds were obtained for the FRM sampler sites from publicly-available databases (13). Filter concentrations were classed as "high" for the purposes of these microscopy comparisons when they were greater than US EPA NAAQS primary standards for 24-hr $PM_{2.5}$ (35 $\mu g/m^3$) or PM_{10} (150 $\mu g/m^3$) (14). Winds were classed as "high" when the 24-hr sampling period exhibited at least one hourly average greater than 20 MPH. PM and wind classifications for all other FRM samples were nominally assigned the value of "low".

Five soil samples from two Imperial Valley locations 2009-2013 were obtained for comparison purposes.

Three UNC Passive PM samplers (RJ Lee Group, Monroeville, PA) were co-located with FRM $PM_{2.5}$ and PM_{10} samplers approximately 2 miles southwest of downtown Phoenix as part of a 2005 U.S. Environmental Protection Agency evaluation of candidate methods for determining PM_{coarse} (PM between 2.5 and 10 μm) (15). The passive sampler collection substrates used were adhesive carbon tabs mounted on 13-mm SEM stubs. Passive samplers were exposed for a period of one week. Seven 24-hr filters were collected sequentially by each FRM sampler during this week, analyzed gravimetrically, and averaged for comparison to the UNC results.

Electron Microscopy

SEM/EDS analyses of the Imperial Valley samples were conducted at California Department of Public Health (CDPH) with an FEI XL30 Environmental SEM with Thermo Fisher Scientific Noran System 7 EDS system. Manual analyses were conducted in an atmosphere of 0.5-1 mBar of water vapor at 20 kV with a back-scattered electron (BSE) and gaseous secondary electron detector (GSE). SI maps were constructed by acquiring images at 4,000x from randomly-chosen locations on each $PM_{2.5}$ and soil subsample and extracting EDS chemistry data from each pixel of these images. The SI maps were used to illustrate the spatial distribution of the major chemical elements, and were also integrated to obtain the average inorganic composition of the particles in each image, after excluding the predominant background elements (fluorine, carbon, and oxygen). For each sample, the average and standard deviation of the results for two SI maps were calculated, and two-tailed t-tests were conducted to identify any statistically significant differences ($p<0.05$) between the elemental compositions. Approximately 20-200 particles were analyzed per sample. PM_{10} filter SI maps were of lesser quality due to more prominent filter matrices and charged,

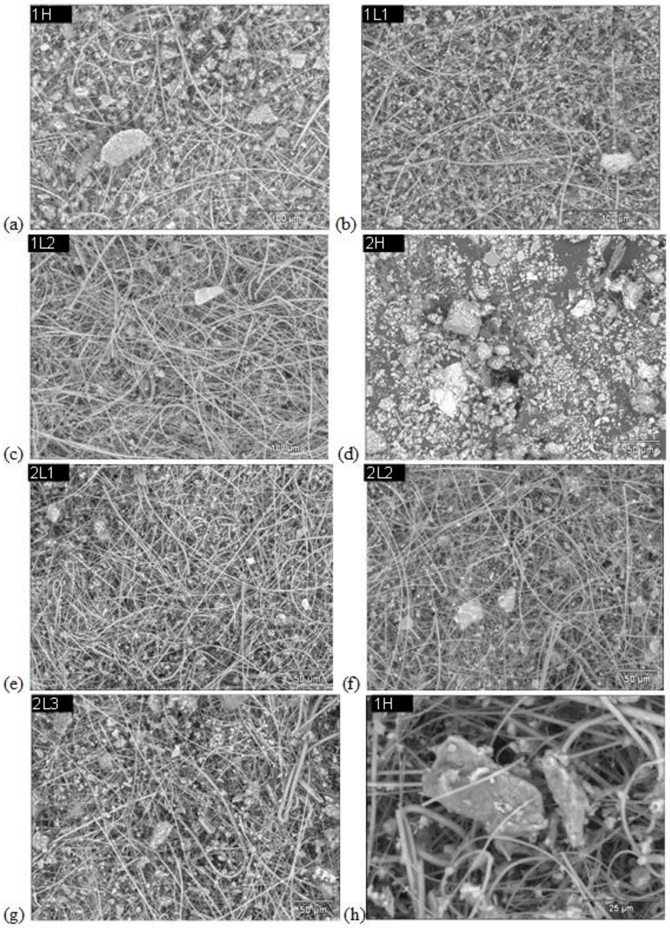

Figure 1. (a)-(g) 600x SEM BSE images from PM_{10} FRM filters (Table 1). Each image is 500 μm wide. Particles > 10 μm are visible in all but are most prevalent in filters 1H and 2H.The very large particles in (d) were removed from the 2H filter matrix before analysis. (h) 2,400x SEM BSE image from filter 1H. Image is approximately 100 μm wide.

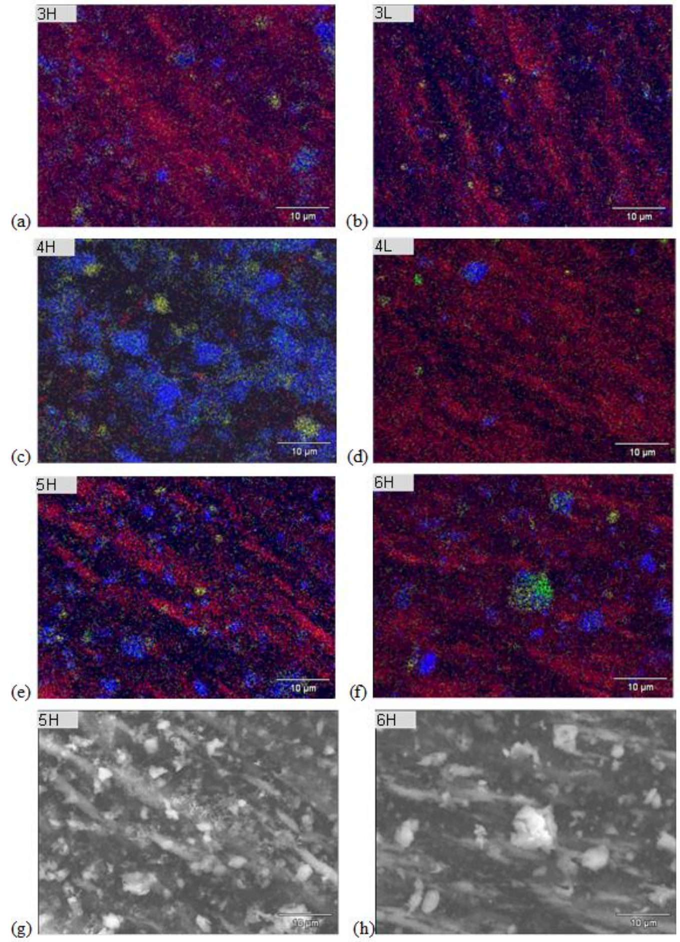

Figure 2. (a)-(f) 4,000x SEM/EDS SI maps from $PM_{2.5}$ FRM filters (Table 1). Width of each image is 80 μm. Many particles > 2.5 μm are visible in 3H, 4H, 5H, and 6H. Si is denoted by blue, Ca is yellow, Na is green, and Fl (indicative of the Teflon filter background) is red. (g)-(h) SE images from same fields as (e)-(f).

loosely-attached surface particles, so these filters were compared using manual SEM/EDS only.

Prior to SEM/EDS analyses, all samples were mounted on adhesive carbon tabs on aluminum stubs and carbon-coated to maximize conductivity. Each Imperial filter subsample was prepared by removing an approximately 1 cm-square section with a clean blade. PM_{10} filter 2H possessed an unusually thick, loosely adhered PM deposit on top of the filter which was transferred with tweezers onto a stub. The relatively small Imperial soil samples (~1 cm^3) were first transferred from glass collection vials to plastic Petri dishes. The finer fraction of the Imperial soil relevant to wind resuspension was then effectively isolated from the larger gravel and sand particles using electrostatic and Van der Waals forces on the underside of each Petri dish lid. This simple technique reduced the maximum observed particle size from approximately 5,000 μm to 25 μm, corresponding roughly to the ISO silt (2-63 μm) and clay (<2 μm) soil fractions (16).

Phoenix UNC Passive PM samples were analyzed by CCSEM/EDS (2) at both RJ Lee Group (RJLG) (ASPEX Personal SEM, Monroeville, PA), and at CDPH using the SEM/EDS system described above. All passive samples were coated with a thin layer of graphitic carbon using vacuum deposition and then analyzed directly in their as-collected condition. The automated analyses produced individual particle projected area and elemental chemistry data, which were compiled and analyzed using a custom Excel template (Microsoft, Redmond, WA) to calculate $PM_{2.5}$, PM_{coarse}, PM_{10}, particle size distributions, and elemental composition pie charts (6).

GIS dust parameter mapping

GIS maps of relevant parameters from the windblown dust literature were generated for the conterminous US using ArcMap (ESRI, Redlands, CA). Publicly available datasets and shapefiles were employed, including reported dust storms 2003-2013 (17), the National Land Cover Database (NLCD) 2006 (18), average annual precipitation 2005-9 (19), Wind Erodibility Groups (WEG) from the State Soil Geographic (STATSGO) Database

(20), cattle and cows per acre 2007 (21), and STATSGO silt fraction (22).

NLCD classes associated with wetlands, forests, and grassland were assumed to be the most protective against wind erosion (24). The remaining NLCD classes, “shrub/scrub”, “barren”, “hay/pasture”, “developed” and “cultivated crops,” possess only partial or intermittent vegetative cover (25), and were assumed to be the most erodible land cover types. The latter three were assumed additionally to be anthropogenically disturbed. Cow density was employed as a first approximation for anthropogenic disturbance on barren and shrub/scrub land, two desert landscapes which otherwise may generate minimal dust (26) (5).

Precipitation was generally assumed to be a dust suppressant, though it can be a confounder when associated with high-wind, summer storms (11) (27).

Unlike some desert regions characterized by coarse, highly erodible sands, Imperial Valley and Phoenix soils primarily consist of finer, silty clays and loams (22). Soil texture (i.e., sand, silt, and clay fractions, and the texture classes defined by their proportions) is treated differently by various dust models. The simplest models consider only the highly erodible sand fraction (>63 μm), though this fraction has not accurately predicted historic dust storms (28), and is much less transportable aloft than the finer silt fraction which tends to dominate windblown dust (23) (29). Other analyses show that wet-sieved, primary particle sizes are often less important than the agglomerated and crusted forms these soils take (30) (31). Nevertheless, soils with high clay and silt fractions appear to generate the highest transportable dust fluxes via saltation (10) (30), especially when anthropogenically disturbed (32) (33) (34) (35). WEG classes containing silty clays are considered moderately erodible due to their tendency to agglomerate into sand-sized particles (23).

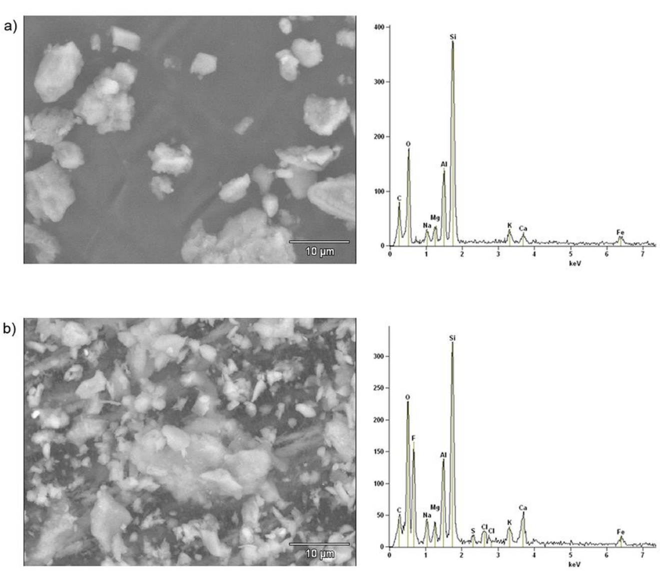

Figure 3. 4,000x SEM BSE images and EDS spectra showing similar morphology and chemistry of silt-sized particles in a) Imperial air on a high-$PM_{2.5}$ day (4H) and b) Imperial soil.

RESULTS

SEM/EDS of Imperial PM Filters and Soils

All high-PM filters were dominated by large, crustal particles which ranged up to 30 μm on the PM_{10} filters (Figure 1) and up to15 μm on the $PM_{2.5}$ filters (Figure 2). These 2-dimensional, physical sizes will be somewhat different than their aerodynamic diameters; observed crustal particles took the form of either thick, flattened plates (Figure 1h) or rounded, near-elliptical grains. SI maps and EDS data from these particles exhibited primarily oxides of silicon or aluminum and silicon, often enriched with calcium and sometimes sodium-chlorine salts (Figures 2-4). The particles also contained minor magnesium, sulfur, and potassium, and occasionally, prominent iron, titanium or barium. The low-PM filters generally possessed fewer large particles than their matched high-PM filters, but otherwise were dominated by particles of a similar, crustal composition. Soil silt fractions exhibited crustal particles with very similar morphology and chemistry to those on the air filters (Figure 3).

Integrated SI maps for two of the high-$PM_{2.5}$ filters revealed higher concentrations of silicon and iron, and lower concentrations of sulfur and chlorine, than their matched low-$PM_{2.5}$ samples (Figure 4). Average differences (high-$PM_{2.5}$ - low-$PM_{2.5}$) for the two filter pairs were +9.8 % silicon (neither difference statistically significant), +4.3% iron (both statistically significant), -8.1 % sulfur (both statistically significant), and -10 % chlorine (one statistically significant). The high-$PM_{2.5}$ filters were consistent with the soil samples, which exhibited even higher concentrations of silicon and iron, and lower sulfur and chlorine. All five soils were very similar to each other for these elements (98% of the 40 pairwise comparisons were statistically

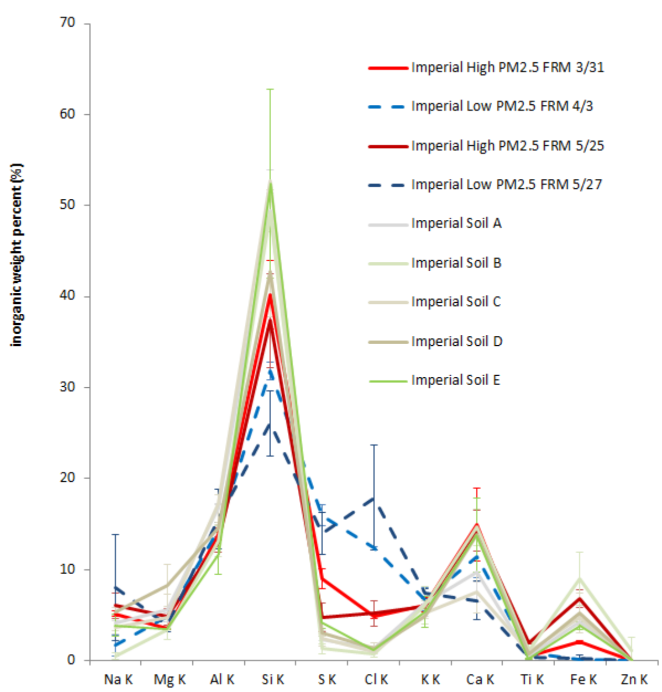

Figure 4. Inorganic element weight percents obtained from EDS SI maps from two high-/low-$PM_{2.5}$ FRM filter pairs and five Imperial County soils. Error bars represent intra-sample standard deviation.

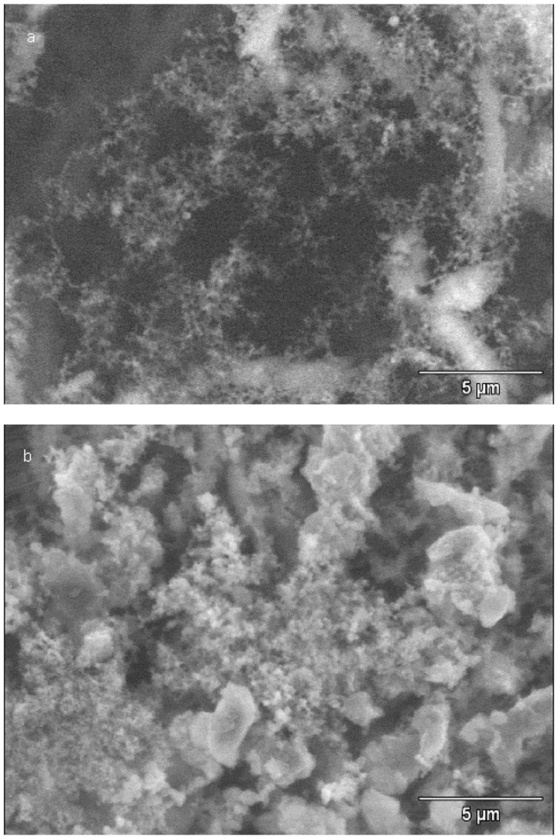

Figure 5. 10,000x GSE ESEM images of soot agglomerates from combustion sources on ImperialFRM $PM_{2.5}$ filters. a) large, isolated soot agglomerate (3L). b) random image from 5H, which exhibited densely agglomerated soot across the entire filter surface.

insignificant). Average differences (soil - low-$PM_{2.5}$) were +20% silicon, +5.2% iron, -12 % sulfur, and -14 % chlorine. Together, these comparisons suggest that the high-$PM_{2.5}$ filters may have contained a higher fraction of regional soil material than the low- $PM_{2.5}$ filters.

The weight percents in Figure 4 are given in terms of percent of inorganic elements only. When carbon and oxygen were included, typical ranges were 15-25% silicon, 0-20% carbon, and 30-50% oxygen, with the other, less prevalent inorganic elements contributing the remainder. These results are consistent with previous bulk X-ray fluorescence (XRF) and thermal/optical reflectance-based PM_{10} filter analyses, which showed that silicon dominated the inorganic composition on high-PM_{10} days in Imperial, with relative concentrations of silicon and total carbon of 14-19% and 7-21%, respectively (36).

Soot agglomerates were also observed in many of the filters, suggesting the influence of combustion sources such as diesel engines or biomass burning (6) (37) (38) (Figure 5). The morphology and composition of these soot agglomerates contrasted strongly with PM from crustal sources. Filter 5H exhibited dense soot agglomerates across the entire surface (Figure 5b).

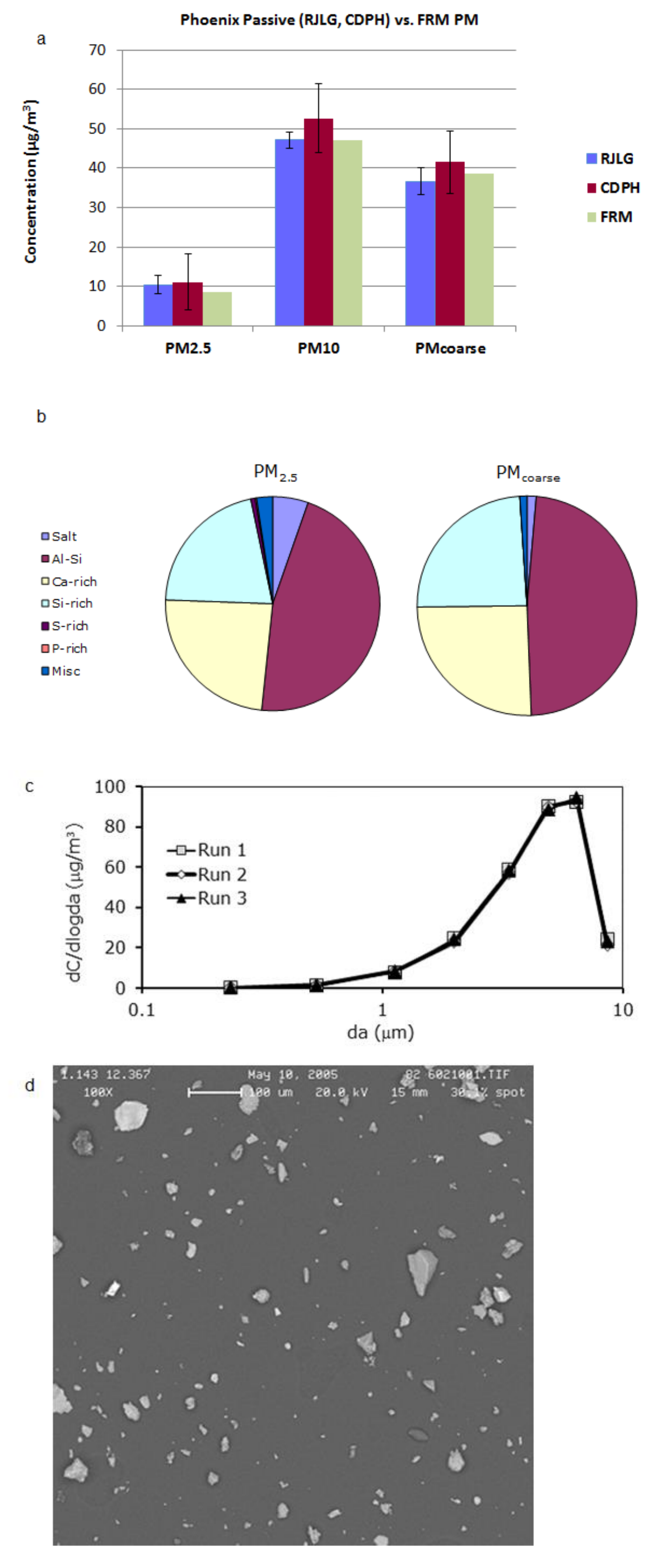

Figure 6. Phoenix UNC Passive PM sampler data. a) PM concentrations from RJLG and CDPH analyses of 1-week passive samples and average of 24-hr FRM data during the same week. Error bars represent the standard deviation of three co-located passive samplers. b) pie chart showing typical passive $PM_{2.5}$ and PM_{coarse} composition from one sample, both dominated by crustal particles. c) typical particle size distributions from triplicate RJLG CCSEM analyses of same passive sample. d) typical BSE image from RJLG CCSEM analysis (100x) showing smooth background and distinct individual particles.

CCSEM/EDS of Phoenix Passive PM Samples

$PM_{2.5}$, PM_{10} and PM_{coarse} from the CCSEM/EDS analyses of the passive samplers agreed well with co-located FRM filter measurements (Figure 6a). Good agreement was also obtained between passive sampler analyses performed at RJLG and CDPH. CCSEM/EDS data revealed mostly crustal compositions in both the fine and coarse PM_{10} fractions, which possessed very similar compositions for these samples (Figure 6b). A typical particle mass size distribution calculated for one passive sample is shown in Figure 6c, with good agreement between triplicate CCSEM analyses conducted by RJLG. Phoenix size distributions were dominated by PM_{coarse}, consistent with a strong crustal influence. Figure 6d shows a typical passive sampler collection density with non-overlapping particles and substrate nearly devoid of obtrusive background structures.

GIS Dust Parameter Maps

Comparing reported dust storms (Figure 7a) to dry, erodible regions (Figure 7d) reveals many correlated regions and no false negatives (FN), i.e., dust storms were only reported in regions predicted to be dusty in Figure 7d. However, several false positives (FP) are observed, i.e., several areas predicted by Figure 7d to be dusty recorded zero dust storms. Refining the prediction map to exclude "undisturbed" barren and scrub/shrub lands (as approximated by cow and cattle data) (Figure 7f) substantially reduces the number of FPs, but yields a notable FN in NE Arizona. Refining the map in Figure 7d to include only those regions with high silt content (Figure 7h) results in several FN predictions, though it achieves improved specificity, with only one major FP in Northwest Utah.

Note that dust storms were reported in both Imperial Valley and Phoenix (Figure 7a), and are also predicted by Figures 7d, 7f, and 7h.

DISCUSSION

Integrated SI maps enabled chemical comparisons between FRM $PM_{2.5}$ filters and soil samples. This technique is analogous in some respects to bulk XRF techniques, which typically integrate PM compositions from air filter areas on the order of 10-100 mm wide (39). The 4,000x SI maps in this study were much smaller, 80μm wide. In addition, the mapping of EDS data to individual image pixels within the SI maps enabled review of selected, individual particles' compositions and sizes down to about 1 μm. SEM/EDS and SI mapping thus produced enhanced information beyond that obtainable by XRF, such as the greater proportion of large crustal particles on high-PM days. Future work will investigate methods to improve SI maps on FRM PM10 filter matrices.

Wind aerosolization and dispersal of coarse and larger PM (2.5-30 μm) is plausible on three of the six high-PM days in Imperial Valley. Winds were much higher on two of the high-$PM_{2.5}$ days and one of the high-PM_{10} days than they were on the matched low-PM days. Although all May 2011 sampling days were relatively windy (Table 1), the day preceding collection of filter 2H was unique in that it exhibited thirteen hours in which wind speeds averaged >20 MPH, resulting in 35 consecutive hours of high winds. Data for the other three high-PM days does not point to unusually high winds, so high-energy regional sources (e.g., local road traffic or construction activity) may have contributed to these high dust levels.

Many of the observed crustal particles were larger than the samplers' nominal cut-point sizes. FRM sampler inlet cleaning or calibration issues could potentially enhance collection of these particles. However, even when operated properly, the S-shaped particle size cut-point curves of the PM_{10} and $PM_{2.5}$ inlets are designed to admit a small but non-zero fraction of particles larger than their nominal cut-points.

The simple dust parameter maps presented in this work show fair correlation and specificity with respect to reported US dust storms, and suggest that Imperial and Phoenix both possess favorable conditions for the creation of airborne dust. Refinements based on anthropogenic disturbances and soil silt content reduced the number of false positives, but failed to predict several regions with observed dust storms. The maps could be improved further with the incorporation of other dust-related parameters such as the unusually low shrub/scrub density in NE Arizona (40) or additional anthropogenic disturbance data. More sophisticated dust erosion models (e.g., WRAP, WEPS, EPIC) are somewhat inconsistent in their dust predictions for Imperial and Phoenix, as are their agreement with the reported dust storms shown in Figure 7a. While computationally quite complex, these models remain somewhat limited in their treatment of anthropogenic disturbances, soil moisture and crusts, transportable PM fraction, and storm events (32) (41) (42) (43). Note that the dust Storm Report data used here depends upon submissions by local residents and organizations, and could conceivably be biased by regional concerns.

The agreement between the UNC Passive PM sampler and FRM data suggests that passive sampling technology can be used to complement FRM samplers in the evaluation of airborne PM. The smooth passive sampler substrates were ideal for automated microscopic examination of individual particles (Figure 7d), which enabled particle size distribution measurements and size-dependent PM concentrations (μg/m^3). CCSEM/EDS thus permitted detailed evaluations in a manner that was not possible on FRM filter samples, which suffered from substantial particle agglomeration and filter matrix interference (Figure 1).

CONCLUSION

Novel analytical, sampling, and GIS mapping approaches were employed to investigate potential sources of PM near two desert cities. SEM/EDS and SI maps of Imperial Valley FRM filters and CCSEM/EDS of Phoenix UNC Passive PM samples point to crustal materials as the main contributor to these PM samples. This crustal PM was readily distinguished via SEM/EDS from combustion PM, the latter of which was observed in substantial amounts on one of the high-$PM_{2.5}$ filters.

Calculated passive PM concentrations in Phoenix agreed well

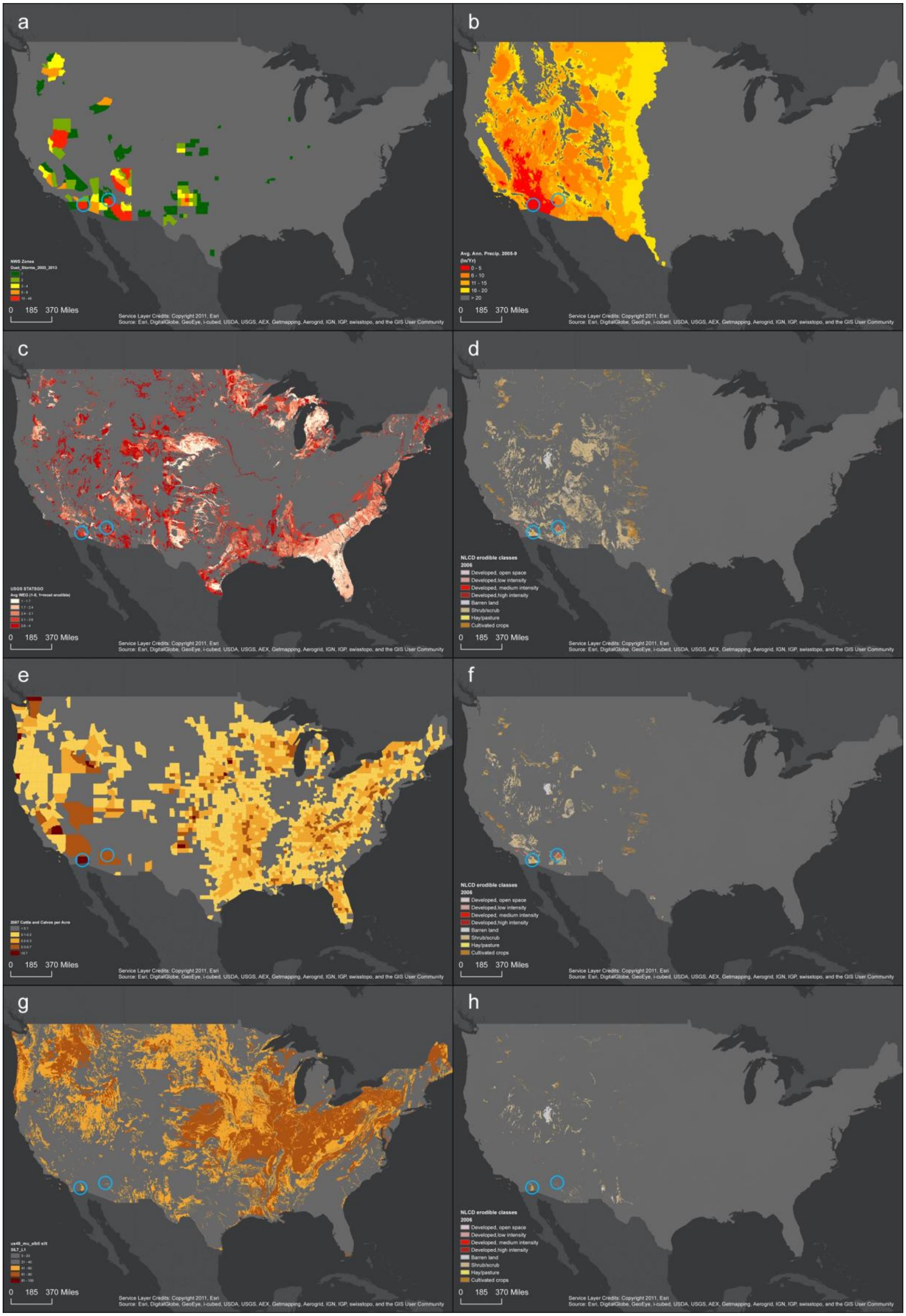

Figure 7. GIS maps of a) reported dust storms, b) dry regions with <20 inches precipitation/year, c) erodible soils with WEG<4, d) erodible land cover (developed, cultivated crops, hay/pasture, barren, or shrub/scrub) intersected with maps (b) and (c), e) >0.1 cows/acre, f) dry, erodible, anthropogenically disturbed regions (same as (d), but only barren and shrub/scrub regions with >0.1 cows/acre) g) >40% silt in top soil layer, h) dry, with erodible regions with silt > 40% (intersection of maps (d) and (g)). The locations of Imperial Valley (left) and Phoenix (right) are circled on each map.

with co-located FRM $PM_{2.5}$ and PM_{10} filter measurements. The UNC Passive PM samplers were better suited for detailed microscopy analyses than the FRM filters, and should be considered as a useful complement to FRM samplers and conventional analytical methods for future investigations of high-PM events. Passive samplers may be especially useful in the evaluation of PM in areas of non-attainment because their low cost permits the deployment of multiple, simultaneous samplers to measure spatial variability.

GIS dust parameter maps support the hypothesis that airborne dust is a feasible source of $PM_{2.5}$ and PM_{10} in Imperial Valley and Phoenix. Although agglomeration and crusting of soils with high silt and clay fractions can limit airborne dust generation, anthropogenic disturbances of these soils when dry may generate high transportable dust fractions.

ACKNOWLEDGMENTS

The authors gratefully acknowledge Roger West and Traci Lersch from RJLG for their work on the CCSEM sample analyses, Tom Merrifield from Merrifield & Associates and Robert Vanderpool from the US Environmental Protection Agency for their assistance in the Phoenix field study, and Stephen Wall from CDPH for helpful advice on the Imperial analyses.

REFERENCES

1. Wagner J, Leith D. Passive Aerosol Sampler. Part I: Principle of Operation. *Aerosol Sci. Technol.* 2001; 34: p. 186-192.
2. Casuccio GS, Janocko PB, Lee RJ, Kelly JF, Dattner SL, Mgebroff JS. The Use of Computer Controlled Scanning Electron Microscopy in Environmental Studies. *Journal of the Air Pollution Control Association*. 1983; 33: p. 937-943.
3. Ault AP, Peters TM, Sawvel EJ, Casuccio GS, Willis RD, Norris GA, et al. Single-Particle SEM-EDX Analysis of Iron-Containing Coarse Particulate Matter in an Urban Environment: Sources and Distribution of Iron within Cleveland, Ohio. *Environ. Sci. Technol.* 2012; 46: p. 4331-4339.
4. US EPA. [Online].; 2013. Available from: http://www.epa.gov/oaqps001/greenbk/mappm10.html.
5. Record FA, Baci LA. Evaluation of the contribution of wind blown dust from the desert to levels of particulate matter in desert communities. US EPA Report. ; 1980. Report No.: EPA-450/2-80-078.
6. Wagner J, Naik-Patel K, Wall S, Harnly M. Measurement of ambient particulate matter concentrations and particle types near agricultural burns using electron microscopy and passive samplers. *Atmospheric Environment.* 2012; 54: p. 260-271.
7. Watson JG, Chow JC. Source characterization of major emission sources in the Imperial and Mexicali Valleys along the US/Mexico border. *Science of the Total Environment.* 2001; 276: p. 33-47.
8. Hagen LJ, Woodruff NP. Air pollution from duststorms in the Great Plains. *Atmos. Environ.* 1973; 7: p. 323-332.
9. Arizona Department of Environmental Quality. Maricopa County PM-10 Serious Area SIP Revision for Agricultural Best Management Practices. ; 2001.
10. Zobeck TM, Amante-Orozco A. Effect of dust source clay and carbonate content on fugitive dust emissions. In *Proceedings of the US-EPA 10th Annual Emission Inventory conference*; 2001.
11. Reheis MC, Urban FE. Regional and climatic controls on seasonal dust generation in the southwestern U.S. *Aeolian Research*. 2011; 3: p. 3-21.
12. Fox TA, Barchyn TE, Hugenholtz CH. Successes of soil conservation in the Canadian Prairies highlighted by a historical decline in blowing dust. *Environ. Res. Lett.*. 2012; 7: p. 014008 (6pp).
13. California Air Resources Board. [Online].; 2013. Available from: http://www.arb.ca.gov/aqmis2/aqdselect.php.
14. US EPA. National Ambient Air Quality Standards (NAAQS). [Online].; 2013. Available from: http://www.epa.gov/air/criteria.html.
15. Willis B, Leith D, Merrifield T, Wagner J, Casuccio GS, Cowley C, et al. Evaluation of PM10, PM2.5, PM10-2.5, Measurements Using a Passive Particulate Sampler. In *AWMA Air Quality Measurements and Technology Symposium*; 2006; Durham NC.
16. ISO. ISO 14688-1. [Online].; 2013. Available from: http://www.iso.org/iso/iso_catalogue/catalogue_tc/catalogue_detail.htm?csnumber=25260.
17. National Climatic Data Center. [Online].; 2013. Available from: http://www.ncdc.noaa.gov/stormevents/ftp.jsp.
18. Fry J, Xian G, Jin S, Dewitz J, Homer C, Yang L, et al. Completion of the 2006 National Land Cover Database for the Conterminous United States. *PE&RS*. 2011; 77: p. 858-864.
19. National Atlas of the United States. United States Average Annual Precipitation, 2005-2009. 2011.
20. Wolock DM. STATSGO soil characteristics for the conterminous United States. 1997; USGS Open-File Report 656.
21. National Atlas of the United States. [Online].; 2010. Available from: http://nationalatlas.gov/mld/agcen07.html.
22. Miller DA, White RA. A Conterminous United States Multi-Layer Soil Characteristics Data Set for Regional Climate and Hydrology Modeling. *Earth Interactions*. 1998; 2: p. 1-26.
23. Gillette DA. Production of dust that may be carried great distances. In Pewe TL,e, editor. *Geol. Soc Am. Spec. Pap.* Desert Dust: Origin, Characteristics, and Effect on Man ed.; 1981. p. 11-26.
24. Floyd K, Gill T. The association of land cover with aeolian sediment production at Jornada Basin, New Mexico, USA. *Aeolian Research*. 2011; 3: p. 55–66.
25. Homer C, Huang C, Yang L, Wylie B, Coan M. Development of a 2001 National Landcover Database for the United States. *Photogrammetric Engineering and Remote Sensing.* 2004; 70: p. 829-840.
26. US EPA. Interim guidance on the preparation of demonstrations in support of requests to exclude ambient air quality data affected by high winds under the exceptional events rule. ; 2013.
27. Bisal F, Hsieh J. Influence of soil moisture on the erodibility of soils by wind. *Soil Science*. 1966; 102: p. 143-46.
28. Cunfer G. Causes of the Dust Bowl. In Knowles AK, editor. *Past Time, Past Place: GIS for History*. Redlands, Calif.: ESRI Press; 2002.
29. Chatenat B, Marticorena B, Gomes L, Bergametti G. Assessing the micropped size distributions of desert soils erodible by wind. *Sedimentology*. 1996; 43: p. 901-911.
30. Alfaro SC, Rajot JL, Nickling W. Estimation of PM20 emissions by wind erosion: main sources of uncertainties. *Geomorphology*. 2004; 59: p. 63–74.

31. King J, Etyemezian V, Sweeney M, Buck B, Nikolich G. Dust emission variability at the Salton Sea, California, USA. *Aeolian Research*. 2011; 3: p. 67-79.
32. Countess Environmental. Methodology for estimating fugitive windblown and mechanically resuspended road dust emissions applicable for regional scale air quality modeling. Final Report for WGA Contract No. 30203-9. Westlake Village, CA:; 2001.
33. Webb N, Strong C. Soil erodibility dynamics and its representation for wind erosion and dust emission models. *Aeolian Research*. 2011; 3: p. 165–179.
34. Baddock M, Zobeck T, Pelt RV, Fredrickson E. Dust emissions from undisturbed and disturbed, crusted playa surfaces: Cattle trampling effects. *Aeolian Research*. 2011; 3: p. 31–41.
35. Aimar S, Mendez M, Funk R, Buschiazzo D. Soil properties related to potential particulate matter emissions (PM10) of sandy soils. *Aeolian Research.* 2012; 3: p. 437–443.
36. Chow J, Watson J. Zones of representation for PM measurements along the US_Mexico border. *Sci. Total Environ*. 2001; 276: p. 49-68.
37. Clague A, Donnet J, Wang T, Peng J. A comparison of diesel engine soot with carbon black. *Carbon*. 1999; 37: p. 1553-1565.
38. Li J, Posfai M, Hobbs P, Buseck P. Individual aerosol particles from biomass burning in southern Africa: 2. Compositions and aging of inorganic particles. *J Geophys Res*. 2004; 108: p. 8484.
39. US Environmental Protection Agency. Guidelines from PM10 Sampling and Analysis Applicable to Receptor Modeling. Research Triangle Park:, Office of Air Quality Planning and Standards; 1994. Report No.: EPA-452/R-94-009.
40. National Resources Conservation Service. NRI Rangeland Resource Assessment—Bare Ground, Intercanopy Gaps, and Soil Aggregate Stability. ; 2010.
41. Hagen LJ. A wind erosion prediction system to meet user needs. *J. Soil and Water Conservation*. 1991; 46: p. 106-111.
42. Mansell G, Lau S, Russell J. Final Report - Fugitive Wind Blown Dust Emissions and Model Performance Evaluation - Phase II. Environ; 2006.
43. Potter SR, Andrews S, Atwood JD, Kellogg RL, Lemunyon J, Norfleet L, et al. Model simulation of soil loss, nutrient loss, and change in soil organic carbon associated with crop production. ; 2006. http://www.nrcs.usda.gov/technical/nri/ceap/croplandreport.